hydroxy-3-naphthoic acid to the methoxy derivative followed by conversion to the isocyanate and then to 2-methoxy-3-naphthylamine. Treatment with SO_2 and Cu yielded the sulfinic acid, which was oxidized with $KMnO_4$ to the sulfonic acid and then treated with aqueous HCl to give 2-naphthol-3-sulfonic acid. This was treated with $NaNO_2$ in aqueous HCl at 0–5 °C and then with sodium perchlorate to yield the sodium salt of 1-nitroso-2-naphthol-3-sulfonate trihydrate. The product was recrystallized from warm water by the addition of ethanol. The details will be published elsewhere.[21]

The ligands were characterized by C,H,N analysis and infrared and proton NMR spectroscopy.

Kinetic Measurements. For the formation kinetics, stock solutions of nickel(II) ($\sim 6 \times 10^{-3}$ M) and ligand ($\sim 6 \times 10^{-5}$ M) were prepared in $LiClO_4$ (0.10 M) and 0.05 M sodium cacodylate, and the pH of each was adjusted by addition of perchloric acid. In the region of pH 3–4.5 only perchloric acid was used to establish the pH. The pH of the solution after mixing in the stopped-flow system was recorded.

For the dissociation kinetics, a stock solution containing $\sim 1 \times 10^{-3}$ M nickel(II) and 1×10^{-5} M ligand in 0.1 M $LiClO_4$ was mixed with the appropriate $LiClO_4$–$HClO_4$ solution in the stopped-flow system. The acid concentration was taken as half of that in the original $LiClO_4$–$HClO_4$ solution.

The reactions were monitored at or near an absorption maximum of the nickel(II) complex. The specific wavelengths for the 3-sulfonate, 4-sulfonate, 5-sulfonate, 7-sulfonate, and 4,6-disulfonate ligands are 446, 455, 436, 440, and 470 nm, respectively.

In each case the reported rate constant is the average of at least five determinations with a range of ±3%.

Instrumentation. The pH was measured with an Orion 801A digital pH meter standardized against appropriate borate, phthalate, and phosphate buffers.[22] The temperature was maintained within ±0.10 °C by water circulating through a double-walled container for the solution.

A Durrum-Gibson D-110 stopped-flow spectrophotometer was used in the absorbance mode, with the output stored on a Biomation 802 transient recorder. The analog unit for subsequent processing is described elsewhere.[23]

The spectral characterization of the ligands were done with a Cary 219 spectrophotometer, a Pye-Unicam SP3-3000 infrared spectrophotometer, and a JEOL JNM-PMX-60 NMR spectrometer. Elemental analyses were performed by the Pascher Mikroanalytisches Laboratorium, Bonn, West Germany.

Acknowledgment. We wish to acknowledge the financial support for this work from the Natural Sciences and Engineering Research Council of Canada and the University of West Indies.

Registry No. $Ni(OH_2)_6^{2+}$, 15365-79-4; 2-nitroso-1-naphthol-4,6-disulfonate, 94517-69-8; 1-nitroso-2-naphthol-3-sulfonate, 94517-70-1; 1-nitroso-2-naphthol-4-sulfonate, 94517-71-2; 1-nitroso-2-naphthol-5-sulfonate, 94517-72-3; 1-nitroso-2-naphthol-7-sulfonate, 94517-73-4.

(21) Bajue, S. A.; Dasgupta, P.; Lalor, G. C., results to be submitted for publication.

(22) Dawson, R. M. C.; Elliot, D. C.; Elliot, W. H.; Jones, K. M. "Data for Biochemical Research", 2nd ed.; Clarendon Press: Oxford, 1969.

(23) Lalor, G. C. *Inorg. Chim. Acta* **1975**, *14*, 179.

Contribution from the Research Laboratories, Eastman Kodak Company, Rochester, New York 14650

Kinetics and Mechanism of Chelation of Nickel(II) by a Tridentate α-[(2-Hydroxyphenyl)azo]-α-acetoacetonitrile and an α-(8-Quinolylazo)-α-acetoacetonitrile Dye

GREGG A. MEYERS, FRANK M. MICHAELS, RICHARD L. REEVES,* and PHILIP J. TROTTER[1]

Received April 18, 1984

The kinetics of formation of 1:1 tridentate chelates with the (2-hydroxyphenyl)azo (**1**) and 8-quinolylazo (**2**) dyes were studied over the pH range 4–9 and at an ionic strength of 0.1 M in buffers that do not complex nickel(II). Resonance-Raman and ^{13}C NMR spectra show that the predominant tautomers of **1** and **2** are the hydrazones at pH < pK_{a1} for **1** (pK_{a1} = 6.11) and at pH < pK_{a2} for **2** (pK_{a2} = 7.32). Ionization at the indicated pK_a's gives the arylazo enolates and eliminates tautomeric forms. Dye **1** has the azo enolate structure in the chelate. The ^1H and ^{13}C NMR spectra show separate lines for conformers that interconvert slowly (τ > 30 ms) at room temperature. Under conditions of neutral and mildly basic pH and excess nickel, an intermediate accumulates, and its formation and decay were measured at wavelengths corresponding to appropriate isosbestic points. Estimated lower limits on the magnitudes of the formation constants for the intermediates indicate that they are bidentate. Rate constants for the final ring-closure step were independent of pH and nickel concentration and had values of 3.7 ± 0.2 and 0.044 ± 0.008 s^{-1}, respectively, for **1** and **2**. Overall formation rate constants for the chelates from the monoanions of **1** and **2** (6.2×10^2 and 1.15×10^3 M^{-1} s^{-1}, respectively) and for the undissociated dyes (<15 and 2.4 M^{-1} s^{-1}, respectively) are much smaller than expected from the water-exchange constant of Ni^{2+} and reasonable outer-sphere formation constants. The slow rates of ring closure and of formation of the intermediates are discussed in terms of steric effects and the presence of unreactive tautomers.

This paper is a continuation of our effort to understand the details of the kinetics and mechanism of the chelation of nickel(II) by tridentate metalizable dyes. In an earlier paper[2] we were able to estimate rate constants for partitioning of partially chelated intermediates from 2-(2-pyridylazo)-1-naphthol (α-PAN) dyes. Whereas one of the ring-closure steps was partially rate limiting, the overall rate constants for formation of 1:1 nickel:dye complexes from the various ionic species of the dyes were only about half the value calculated from the water-exchange rate of Ni^{2+} and reasonable values for the outer-sphere complex constant. We also showed that the 1:2 nickel:dye complex (MD_2) of the α-PAN dyes forms surprisingly rapidly from the 1:1 complex (MD) via a consecutive competitive pathway. Initial chelation gives a kinetically controlled mixture of complexes in which the 1:2 complex exceeds its equilibrium concentration. We suggested that complexation of the first dye served as a template to facilitate rapid addition of a second dye, following the concept advanced by Cayley and Margerum.[3]

In this paper we have sought to extend the generality of the earlier findings. Dyes **1** and **2** were selected for several reasons: (a) The dyes have fewer and smaller aromatic moieties than the α-PAN dyes and were expected to differ in their ability to form templates for facilitating 1:2 complex formation. (b) Space-filling

(1) Present address: Coherent, Inc., Palo Alto, CA 94304.

(2) Reeves, R. L.; Calabrese, G. S.; Harkaway, S. A. *Inorg. Chem.* **1983**, *22*, 3076.

(3) Cayley, G. R.; Margerum, D. W. *J. Chem. Soc., Chem. Commun.* **1974**, 1002.

0020-1669/85/1324-0731$01.50/0

Table I. Structural Forms of Dye 1 with Respect to pH and Nickel Complexing

soln	pH[a]	principal Raman bands, cm^{-1} C=O	aryl (Ar)	N=N	azo bridge	Ar-O str	structure
dye	4.5	1665 mw	1603 m	not obsd	not obsd	1258 w	hydrazone form (structure A)
dye	8.0		1600 m	1369 vs	-----1185-----1230----- broad, strong, coalesced		azo anion (with Ar-OH shifted) (structure D)
dye	13.0		1578 mw	1376 vvs	1178 s	1246 s	azo dianion (with Ar-O^- and "free" azo bridge)
dye-Ni (1:1)	4, 8, 13[b]		vw	1411 vvs	1178 s	1250 s	dye-Ni complex (structure F)

[a] In water $pK_{a1} = 6.11$ and $pK_{a2} = 10.14$. Studies were done in H_2O and D_2O. The pH was adjusted with KOD or NaOH and HCl in unbuffered solutions, and the pH of each solution for Raman study was measured independently. [b] At pH 4, the dye-Ni (1:1) solution was in equilibrium between the dye-Ni complex and the protonated hydrazone; at pH 8 and 13, the dye was fully metalized.

models suggested that **1** and **2** have steric constraints for chelation that are different from those of the α-PAN dyes. (c) The dyes can exist in several tautomeric forms (Scheme I), and we wanted to assess the importance of the tautomerism on the kinetics of chelation.

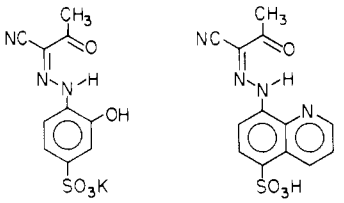

1 **2**

We find no evidence for kinetically controlled formation of 1:2 complexes with these dyes. We do find that final ring closure is relatively slow so that intermediates accumulate and their rates of formation and decay can be studied. The low reactivity of the various ionic forms of the dyes is attributed to a combination of sterically unfavorable conformations and the presence of unreactive tautomers.

Experimental Section

Materials. The purification of the two dyes is described in the accompanying paper.[4] The *N*-morpholineethanesulfonic acid (MES) and *N*-(2-hydroxyethyl)piperazine-*N'*-propanesulfonic acid (HEPPS) buffers were the same as those described earlier.[2] *N*-(2-Hydroxyethyl)-piperazine-*N'*-ethanesulfonic acid (HEPES) was Fluka puriss. grade and was used as received. The preparation of the nickel perchlorate stock solution was described earlier.[2]

Instrumentation and Methods. Raman spectra were recorded on a Cary Model 82 Raman spectrometer. A Spectra-Physics (S-P) Model 165 krypton ion laser provided excitation at 647.1 nm. An S-P argon laser was used to cover the 454.5–514.5-nm excitation range. A Coherent Radiation Model 590 dye laser provided tuning in the 575.0–640.0-nm excitation range.

Resonance-Raman enhancement allowed dye solutions to be measured in the 10^{-3}–10^{-7} M concentration range. The following settings were generally optimum: 5-cm^{-1} bandwidth, 10-s pen period, 1000 or 2000 counts/s sensitivity. With the solutions, maximum excitation intensity was achieved by placing the sample in a 1-mm capillary tube aligned so that the laser beam passed through the center of the sample along the full 2-cm sample column. A wide range of laser excitation was required to optimize resonance-Raman signal output vs. visible absorption. This laser tuning is provided in the visible region by the Model 590 jet-stream dye laser. Rhodamine-6G laser dye was pumped with ~3–4 W (sum of all lines) from the argon gas laser. The large amount of collimated background fluorescence emission from the dye laser required the use of a premonochromator filtering system prior to sample irradiation. Modifications were made in the laser-line filtering system to obtain excitation from any single line between 450 and 680 nm. A large number of fluorescent plasma emission lines from the laser gas must also be eliminated. Resonance-Raman intensity enhancements could be observed by utilizing several laser wavelengths falling in the region of dye absorption.

The ^{13}C NMR spectra were obtained with a Bruker WH270 spectrometer with a 10-mm probe. The variable-temperature ^1H NMR spectra were obtained with an IBM WP27054 spectrometer and a 5-mm probe.

(4) Reeves, R. L.; Maggio, M. S.; Harkaway, S. A.; Meyers, G. A. *Inorg. Chem.*, following paper in this issue.

Scheme I

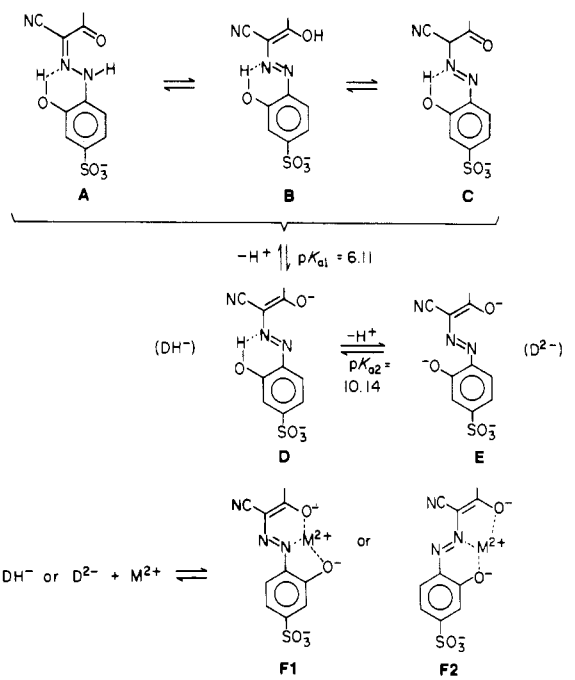

The rapid kinetic measurements were made at 25 °C on a Durrum stopped-flow spectrophotometer interfaced with an On Line Instrument System (OLIS) Model 3820 data system. Several records were averaged in the determination of each rate constant. After each averaged experimental trace was fitted in an exponential form, residuals were examined by a point-by-point subtraction of the calculated trace from the experimental trace. A lack of fit was signaled by a pattern in the residuals. In such cases, a smaller segment of the experimental trace was selected for fitting by eliminating data from the later stages until the residuals for the selected segment were random. In nearly all cases, random residuals were less than ±0.002 absorbance unit.

The slower runs were monitored on a Cary 118C recording spectrophotometer. Rates were monitored at a single wavelength with the chart drive used as a time base, or spectra were recorded as a function of time by use of a programmer and a repetitive scan device.

Absorption curves as a function of reaction time were generated in stopped-flow experiments in which averaged traces of absorbance vs. time were recorded on a grid for a series of wavelengths at 10-nm intervals. Absorbance–wavelength coordinates were taken from the various plots for specified elapsed times to generate absorption curves for those times.

Results

Acid–Base and Tautomeric Equilibria. Stability constants and absorption curves of the 1:1 and 1:2 nickel:dye complexes of **1** and **2** are given in the accompanying paper.[4] Experimental dissociation constants and possible tautomeric forms of dye 1 are shown in Scheme I. The charges shown on the DH_i species refer to the charges on ligand groups only. Similar tautomeric structures can be drawn for the DH species of **2**. The pK_{a2} for dissociation of the DH species of **2** is 7.32. Dissociation of the quinolinium species (DH_2^+) of **2** occurs below pH 4 where complexation is insignificant. Each of the tautomers **A**–**C** could be kinetically distinct entities, but under equilibrium conditions the tautomeric mixture will ionize as a single species. Under conditions of rapid

chelation, tautomer C could ionize more slowly than the rate of chelation.

Raman spectra of dye **1** were obtained at different steps of dissociation. The principal Raman bands, their assignments, and the deduced structures of the predominant species are given in Table I.

At pH 4.5 dye **1** shows no azo vibrations and exists predominantly as the hydrazone form (structure **A**).[5] At pH 8.0, the spectrum shows a loss of the C=O band and formation of N=N.[6-8] This implies removal of the hydrazone proton at pH = pK_{a1} to form structure **D**. Indirect evidence for a hydrogen bond between the phenolic OH and an azo nitrogen is obtained from the shift of the Ar–O stretching and azo-bridge[6,7] bands to yield broad coalescence at 1230–1185 cm^{-1}. When the phenolic OH is ionized at pH 13, the coalesced band of structure **D** splits into separate Ar–O (1246 cm^{-1}) and azo-bridge (1178 cm^{-1}) bands, and the D^{2-} dye species has structure **E**.

The 1:1 nickel:dye complex of **1** was formed in situ by addition of a 10-fold excess of Ni^{2+} to the dye solution[4] and was examined by the resonance-Raman technique. Intense bands at 1410 and 1408 cm^{-1} were observed at pH 8 and 11, respectively, for the complexed azo–Ni vibration and were well resolved from other bands. These bands have higher frequencies than those of uncomplexed azo bands (1370 and 1378 cm^{-1} at pH 8.3 and 11.3, respectively), which indicates a higher N=N bond order in the complexed dye.

The Ar–O stretching was shifted to 1250 cm^{-1} upon complexing at all pH values, but the azo-bridge band at 1179 cm^{-1} was unchanged. The C=O band was eliminated upon complexing. The complex has the azo enolate structure. Structures **F1** and **F2** show the two possible azo enolate forms of the complex.

The ^1H and ^{13}C NMR spectra of **1** were measured in 50% (v/v) D_2O–Me_2SO at acidic, neutral, and basic pH and generally confirmed the structure assignments deduced from the Raman data. In addition, the NMR results on **1** showed the presence of several conformers that interchange slowly on the NMR time scale. At acid pH extra peaks are observed in both the ^1H and ^{13}C spectra. The bands in the ^1H spectrum of this solution coalesced at 60 °C, and the spectrum became that of a single component. The extra peaks are due either to slowly equilibrating tautomers or to hindered internal rotation. The ^{13}C spectrum of the neutral solution showed fewer bands than the acid solution, and these were broadened.

The ^1H NMR spectrum of completely dissociated **1** in basic solution showed four peaks for the methyl protons instead of the expected singlet. Two intense peaks fell at 2.48 and 2.45 ppm, and two weak bands (one-eighth the intensity of the stronger ones) fell at 2.34 and 2.32 ppm. We interpret this to be the result of two slowly interconverting conformations of the methyl group in two conformations involving other bonds of the dye. On heating, the weaker peaks coalesced with the stronger ones at 60 °C. The two stronger peaks were not completely coalesced at 100 °C. From the frequency difference of the stronger peaks at room temperature we calculated a minimum lifetime τ of the methyl group in either environment of $\tau > 30$ ms.[10]

Initial Products of Chelation. The stability constants for MD and MD_2 complexes of both dyes[4] require that MD be the predominant product at equilibrium in a 10-fold excess of nickel(II). The absorption curve of the initial chelation product of dye **2**, measured after several minutes, was that of the 1:1 complex, and there was no further equilibration following the initial rapid reaction. A slow equilibration did follow the initial rapid complexation of **1**. In a pH 8.72 Tris buffer the stable MD complex has maximum absorption at 442 nm, whereas the initial chelation product had maximum absorption at 448 nm. The initial product was slowly converted to the stable MD complex with an isosbestic point at 445 nm and a first-order rate constant of 2.4×10^{-4} s^{-1}. The spectral change during the slow equilibration did not correspond to the change associated with various ratios of the 1:1 and 1:2 complexes. Equilibrated solutions containing various ratios of MD and MD_2 had isosbestic points at 396 and 453 nm in the pH 8.72 Tris buffer. We have no evidence that the MD_2 complex from either dye forms rapidly and competitively in an excess of nickel(II). We believe that the initial product from **1** is an unstable 1:1 complex that is isomeric with the stable 1:1 complex (see Discussion).

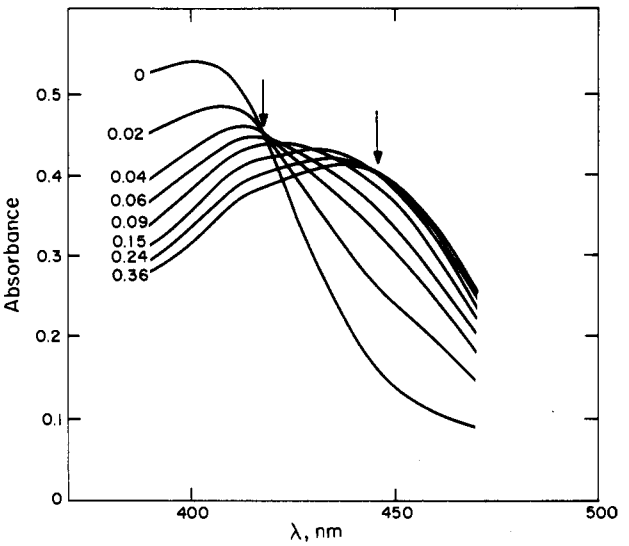

Figure 1. Constructed absorption curves as a function of reaction time for reaction of **1** (1.0×10^{-5} M) with 0.01 M nickel perchlorate in pH 8.04 HEPPS. I = 0.1 M ($NaClO_4$); T = 25 °C. Elapsed times in seconds, uncorrected for the dead time, are indicated. At 0.09 s ~70% of the initial dye is present as the intermediate.

Kinetics of Chelation. The kinetic and spectral results that follow refer to the rapid (stopped-flow) changes that lead to the sole product from **2** and to the first product from **1**, which were described above. At a constant excess, but low concentration, of nickel and neutral or acidic pH, chelation of **1** followed pseudo-first-order kinetics. The experimental rate constants were proportional to the nickel concentration in a moderate excess of nickel and were independent of the wavelength of measurement. Under these conditions we may assume that there is no accumulation of intermediates, and we designate these as "steady-state" conditions. Increasing the pH and nickel concentration gave biphasic kinetics at most wavelengths with the apparent rate constants for the two first-order relaxations being somewhat wavelength dependent. Under such conditions an intermediate accumulates and makes differential contributions to the total absorbance change at different wavelengths. The intermediate decays in less than 1 s.

At a dye concentration of 1×10^{-5} M and nickel concentration of 1×10^{-4} M, steady-state conditions prevail for dye **1** up to pH 7.8. There is significant accumulation of intermediate under these concentration conditions at higher pH and at pH <7.8 at higher nickel concentrations. An intermediate from dye **2** accumulates at pH as low as 6.2 under the specified concentration conditions.

Figure 1 shows absorption curves as a function of reaction time for the chelation of **1** in 0.01 M nickel perchlorate at pH 8.0. Under these conditions, 70% of the initial dye is present as intermediate after 90 ms. The curves show an isosbestic point between the curves of dye and intermediate at 418 nm during the very early stages of reaction before the product appears. There is a second isosbestic point at 446 nm between the curves of the intermediate and product that appears during the final stages of reaction when no dye remains. At this isosbestic point the absorbance change is proportional to the conversion of dye to in-

(5) Trotter, P. J. *Appl. Spectrosc.* **1977**, *31*, 30.
(6) Hacker, H. *Spectrochim. Acta* **1965**, *21*, 1989 and references therein.
(7) Brandmuller, J.; Hacker, H. *Z. Phys.* **1965**, *184*, 14.
(8) Kode, S.; Udagawa, Y.; Mikami, N. Kaya, K.; Ito, M. *Bull. Chem. Soc. Jpn.* **1972**, *45*, 3542.
(9) Giannini, D., unpublished results from the Kodak Research Laboratories.
(10) Drago, R. "Physical Methods in Chemistry"; W. B. Saunders: London, 1977; p 86.

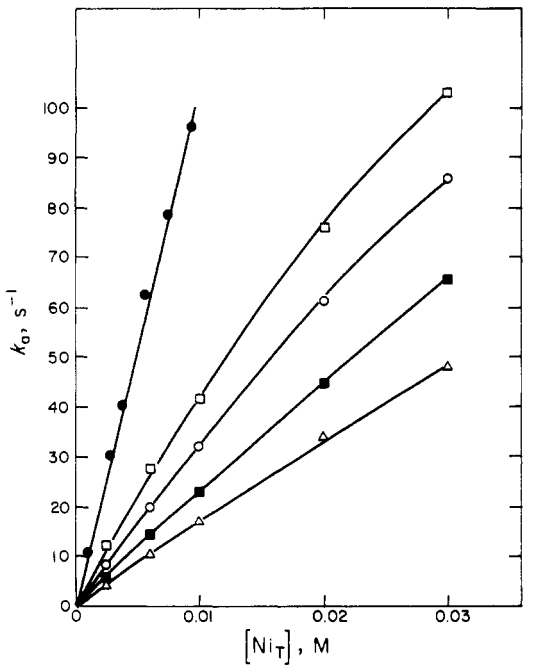

Figure 2. Pseudo-first-order rate constants for the formation of the intermediate from dye **1** as a function of the stoichiometric nickel concentration in HEPPS buffers: Δ, pH 7.24; ■, pH 7.68; O, pH 8.11; □, pH 8.51; ●, pH 9.12. T = 25 °C; $[B^-]$ = 0.01 M; I = 0.1 M. The rates were monitored at the 446-nm isosbestic point.

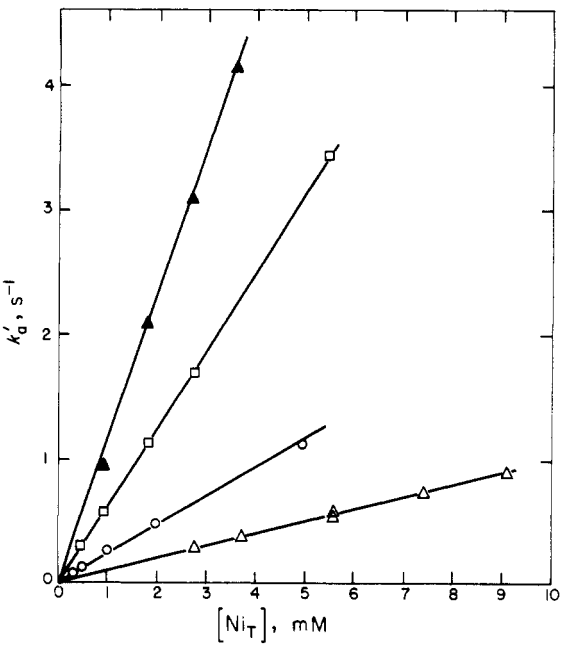

Figure 3. Pseudo-first-order rate constants for the formation of the intermediate from dye **2** as a function of the stoichiometric nickel concentration: Δ, pH 6.27 MES; O, pH 6.68 MES; □, pH 7.33 HEPPS; ▲, pH 8.31 HEPPS. T = 25 °C; $[B^-]$ = 0.01 M; I = 0.1 M. The rates were monitored at the 441-nm isosbestic point.

termediate (k_a). With dye **2**, the isosbestic point in the curves of intermediate and product fell at 441 nm. The isosbestic point in the curves for dye and intermediate shifted with pH between 406 and 412 nm at pH near the pK_a for the dye.

We established that the second spectral relaxation in the complexation of **1** was the result of an accumulated intermediate and not the result of a rapid equilibration of 1:2 complex formed during the initial reaction[2] by preparing the 1:2 complex in situ and observing the spectral changes that resulted upon treatment with excess nickel(II). Equilibration of dye and 0.5 equiv of nickel in unbuffered base at pH 11.1 gave the 1:2 complex, as confirmed by the absorption curve.[4] Treatment of the complex with a 10- to 100-fold excess of nickel perchlorate in a pH 8.4 Tris buffer gave no significant spectral change at the 418-nm and 446-nm isosbestic points during times when the intermediate from **1** forms and decays.

The accumulation and decay of the intermediate X was analyzed by eq 1. The absorbance changes at the long-wavelength

$$M + D \underset{k_{-a}}{\overset{k_a}{\rightleftharpoons}} X \xrightarrow{k_b} MD \qquad (1)$$

isosbestic points, corresponding to the conversion of D to X, was first order throughout the change with **1** and for about 80% of the change with **2**, when the concentration of nickel(II) was in constant excess. The pseudo-first-order rate constants k_a' ($k_a' = k_a[M]$) varied with the nickel concentration. Figure 2 shows plots of k_a' for **1** as a function of the stoichiometric nickel concentration $[Ni_T]$. Figure 3 shows similar plots for **2**. With **1**, the values of k_a' are proportional to $[Ni_T]$ at the lower concentrations. Curvature develops at the higher concentrations and higher pH because of the presence of hydrolyzed or multinuclear nickel species. Values of k_a obtained from the slopes of the linear segments of the plots are listed in Table II. The k_a' values for **2** could be measured at lower nickel concentrations than for **1**, and k_a' is strictly proportional to $[Ni_T]$ (Figure 3). The derived k_a values are listed in Table II.

The plots of k_a' vs. $[Ni_T]$ for both dyes had zero intercepts, showing that k_{-a} in eq 1 is negligibly small. In an excess of nickel, eq 1 then reduces to two consecutive first-order reactions. Figure 4 shows a trace obtained at the 418-nm isosbestic point for dye **1**, corresponding to the conversion of X to MD. Similar traces were obtained at the short-wavelength isosbestic points of **2**. The zero-amplitude induction period corresponds to the lifetime of the isosbestic point, i.e., the period during which the dye and the intermediate are the only two absorbing species. Under conditions where $k_a' \geq 10k_b$, the two steps in the sequence are sufficiently separated in time that the absorbance change beyond the maximum rate is proportional to the conversion of X to MD. The superposition of the fitted exponential curve and the experimental

Table II. Rate Constants for the Formation and Decay of Intermediates[a,b]

pH	$[Ni_T]$, mM	$10^{-3}k_a$, M^{-1} s^{-1}	k_b, s^{-1}
		Dye 1	
7.24	20	1.7	3.8
	30		3.8
7.68	10	2.3	3.6
	20		3.8
	30		3.8
8.11		3.0	
8.51	6	5.0	3.6
	10		3.7
	20		3.7
	30		3.8
8.67		6.6	
9.12		10.9	
k_b ± 95% confidence limits = 3.7 ± 0.2 s^{-1}			
		Dye 2	
6.27[c]		0.097	
6.68[c]	2	0.23	0.044
	5		0.047
	10		0.040
7.33		0.61	
7.33[c]		0.61	
7.52	1		0.044
	2		0.044
	5		0.041
	10		0.047
7.82		0.89	
8.31		1.08	
k_b ± 95% confidence limits = 0.044 ± 0.008 s^{-1}			

[a] HEPPS buffers except where noted. [b] T = 25 °C; $[B^-]$ = 0.01 M; I = 0.1 M. [c] MES buffer.

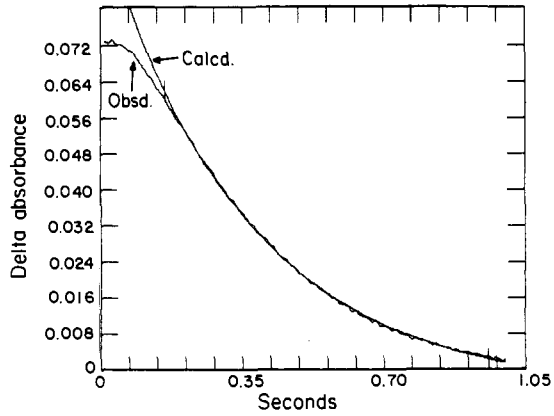

Figure 4. Absorbance as a function of reaction time at the 418-nm isosbestic point, corresponding to the conversion of the intermediate from **1** to the product. Conditions: pH 7.24 HEPPS; 6 mM nickel; 25 °C; I = 0.1 M.

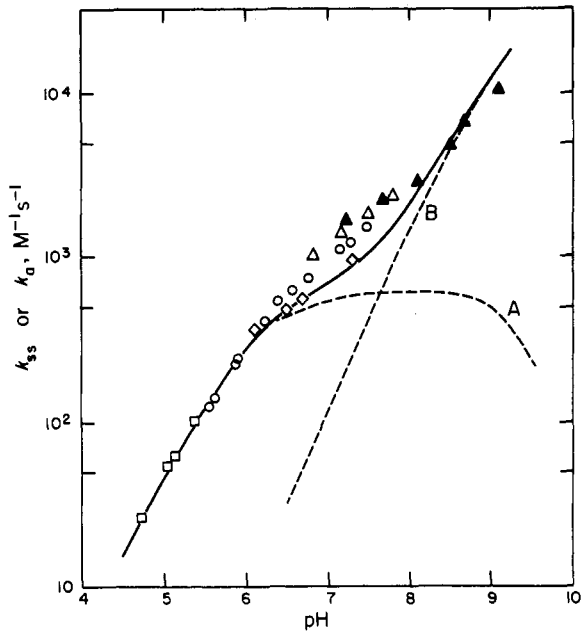

Figure 5. Semilog plot of k_{ss} (open points) or k_a (solid points) for dye **1** as a function of pH: □, acetate; ○, MES; △, HEPES or HEPPS; ◇, extrapolation to zero buffer concentration in a series of MES buffers, Figure 6. T = 25 °C; [B^-] = 0.01 M; I = 0.1 M. The continuous line was calculated with eq 4 and the rate constants from Table III. Dashed curve A: $k_{Ni^{2+},DH^-}f_{Ni^{2+}}f_{DH^-}$. Dashed curve B: $k_{Ni^{2+},D^{2-}}f_{Ni^{2+}}f_{D^{2-}}$.

curve beyond the maximum rate confirms the first-order nature of this conversion. Precise values of k_b were obtained by this fitting method under the stated conditions as shown in Table II.

Effect of Buffer and pH. Second-order rate constants for formation of the product from **1** under steady-state conditions, k_{ss}, were measured over the pH range 4.7–7.8. At the lowest pH, complexation was incomplete, and the rate constant for the forward reaction was obtained from the slope of a plot of k_{obsd} vs. [Ni_T]. Second-order rate constants for the formation of the intermediate from **1**, k_a, were measured in the pH range 7.2–9.1. Since the intermediate partitions almost entirely in the forward direction ($k_b >> k_{-a}$), the rate-determining step under steady-state conditions should be the formation of the intermediate so that k_{ss} and k_a should be equal. Figure 5 shows a plot of the two constants obtained in various buffers containing 0.01 M buffer anion. The plot shows that, in a given buffer, k_{ss} and k_a are equal in the pH range where both constants were measured. We found, however, that k_{ss} for **1** was consistently higher by 20–30% in HEPPS and HEPES buffers than in MES buffers at the same pH and buffer ion concentration. We also found that the absorption curve of **1** had a 3% higher absorptivity in a pH 7.3 HEPPS buffer ([B^-] = 0.02 M, I = 0.1 M) than in an MES buffer of the same pH and composition or in 0.1 M sodium perchlorate at pH 7.3.

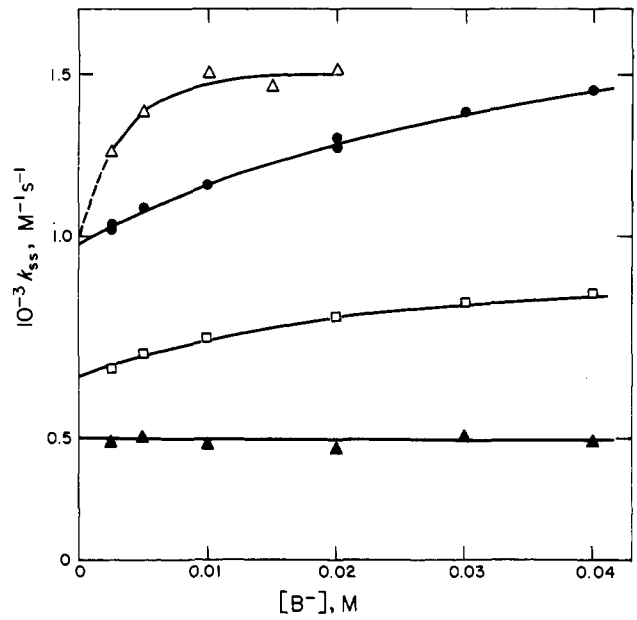

Figure 6. Plots of k_{ss} for dye **1** as a function of the concentration of buffer anion: △, HEPPS, pH 7.30 ± 0.01; ●, MES, pH 7.26 ± 0.04; □, MES, pH 6.69 ± 0.02; ▲, MES, pH 6.12 ± 0.02. T = 25 °C; I = 0.1 M.

Table III. Specific Rate Constants for the Chelation of Ni^{2+} by the Various Ionic Species of the Dyes[a]

	$k_{Ni^{2+},D}$, M^{-1} s^{-1}	k_{Ni^{2+},D^-}, M^{-1} s^{-1}	$k_{Ni^{2+},D^{2-}}$, M^{-1} s^{-1}
1	<15	6.2×10^2	2×10^5
2	2.4	1.15×10^3	
7	1.8×10^3 [b]	4.0×10^4 [b]	

[a] 25 °C; I = 0.1 M. [b] From ref 2; I = 0.04 M.

Values of k_{ss} for **1** were measured as a function of buffer concentration at constant pH, and the results are shown in Figure 6 (plotted vs. the concentration of buffer anion). There is a small kinetic effect from the buffer at pH ≥6.7 that depends upon the nature of the buffer. The larger effect in HEPPS buffer reaches a saturation value at relatively low buffer concentration so that extrapolation to zero buffer concentration in this buffer is not feasible. Extrapolated values could be obtained in MES buffers, and these are shown as diamonds in Figure 5.

The nonlinear effect of the buffers and the direction of the change in slope with pH in MES buffers (Figure 6) argue against general-acid–general-base catalysis by the buffers. The kinetic effects coupled with the spectral results in the absence of nickel ion makes specific pH-dependent complexing between dye ad buffers more likely. The absence of a buffer effect in the reaction of α-PAN dyes[2] suggests that the kinetic effect with **1** does not involve complexing between the buffer and nickel(II) species.

The absorption curves of **2** at pH 7.3 in 0.1 M sodium perchlorate and MES buffer (I = 0.1 M, [B^-] = 0.02 M) were identical. The curve in a HEPPS buffer under the same conditions was slightly red-shifted, and the absorptivity at the maximum was increased by 3%. At a given pH and a buffer anion concentration of 0.01 M, however, values of k_a measured in MES and HEPPS were identical.

In the pH range 4–8.5 the effect of pH on the chelation rates can be described in terms of the reaction of Ni^{2+} with the various ionic species of the dyes. The terms contributing to the rate equation for **1** are derived from eq 2 and 3. The experimental

$$DH^- + Ni^{2+} \longrightarrow MD + H^+ \quad k_{Ni^{2+},DH^-} \qquad (2)$$

$$-H^+ \uparrow\downarrow +H^+$$

$$D^{2-} + Ni^{2+} \longrightarrow MD \quad k_{Ni^{2+},D^{2-}} \qquad (3)$$

second-order rate constants are given by eq 4, where f_{DH^-} and $f_{D^{2-}}$

$$k_{ss} = k_a = f_{Ni^{2+}}(k_{Ni^{2+},DH^-}f_{DH^-} + k_{Ni^{2+},D^{2-}}f_{D^{2-}}) \quad (4)$$

are the fractions of the total dye present as DH^- and D^{2-}, respectively (Scheme I), and $f_{Ni^{2+}}$ is the fraction of the total nickel(II) present as Ni^{2+}. A more detailed derivation was given earlier.[2] The continuous line shown in Figure 5 was calculated via eq 4, and the contributions from the separate terms are shown as dashed lines. The k_{ij} values used for the fit are collected in Table III.

In the designation of the rate constants in the table, the protons on the dye species are omitted and only the ligand charges are indicated. Thus the D^- species is DH^- for **1** and D^- for **2**. A contribution from a term involving the DH_2 species of **1** was undetectable in the accessible pH range. The upper limit for k_{Ni^{2+},DH_2} was estimated from the value the rate constant would need to have to cause detectable curvature in the log k–pH profile at low pH.

The second increase in the rate constant with pH beyond the inflection in the profile is ascribed to the reaction of Ni^{2+} with D^{2-} rather than to a kinetically equivalent contribution from reaction of $NiOH^+$ with DH^-. The two contributions are indistinguishable kinetically since Ni^{2+} dissociates to $NiOH^+$ in the same pH region where DH^- dissociates to D^{2-}. The required rate constant (2×10^5 M^{-1} s^{-1}) seems too large for a reaction between DH^- and $NiOH^+$, however, since it would require either a very large water-exchange rate in $NiOH^+$ or an unexpectedly large outer-sphere complex constant. In addition, it would make $NiOH^+$ more reactive toward DH^- than Ni^{2+} by a factor of 300, whereas in earlier work we[2] and others[11] have estimated that $NiOH^+$ is more reactive than Ni^{2+} toward a given dye species by a factor of 5–7.

The effect of pH on the experimental second-order rate constants for **2** is given for eq 5. The continuous line through the

$$k_{ss} \simeq k_a = f_{Ni^{2+}}(k_{Ni^{2+},DH}f_{DH} + k_{Ni^{2+},D^-}f_{D^-}) \quad (5)$$

data points in Figure 7 was calculated by fitting the points by eq 5. The values of the rate constants required for the fit are given in Table III. Since this dye is almost totally ionized above pH 8.5, measurements made at pH 9–11 should provide information on the rates of complexation of hydrolyzed nickel species with the dissociated dye. Attempts to make such measurements failed because the dye is so unreactive that above pH 9.5, precipitation of nickel hydroxide competed with chelation.

Effect of Ionic Strength. The effect of ionic strength on the chelation of Ni(II) by **2** was measured in a pH 8.6 buffer. At this pH the only contribution to the measured rate is from the reaction of Ni^{2+} with completely dissociated dye, D^-. The total ionic strength was made up of contributions from the buffer anion (1 mM), nickel perchlorate (0.2 mM), and added sodium perchlorate. A plot of log k_a vs. $I^{1/2}$ was linear over a range of I values from 1.6 to 50 mM (Figure 8). A value of −1.85 for the product of the ion charges, $Z_{Ni^{2+}}Z_D$, was obtained from the slope, from which we conclude that the effective charge on the dye is close to 1−. The result shows that only the ligand charge is affecting the rate, and the remote diffuse charge on the sulfonate group is not being sensed. It was noted earlier that remote nonligand charged groups have little effect on ligation rates.[2,12]

Discussion

The results are interpreted in terms of the generally accepted multistep sequence for chelation (eq 6–9) where L–L–L represents the tridentate dye. Under conditions where the steady-state approximation applies to the unidentate and bidentate intermediates **5** and **6** the second-order rate constant for formation of MD is given by eq 10, which was derived by assuming that k_{-3} is negligible.

$$\underset{3}{(H_2O)_6M^{2+}} + L\text{-}L\text{-}L \rightleftharpoons \underset{4}{(H_2O)_6M\cdot L\text{-}L\text{-}L} \qquad K_0 = \frac{[4]}{[3][L\text{-}L\text{-}L]} \quad (6)$$

$$\underset{4}{} \overset{k_1}{\underset{k_{-1}}{\rightleftharpoons}} \underset{5}{(H_2O)_5M\text{-}L\text{-}L\text{-}L} + H_2O \quad (7)$$

$$\underset{5}{} \overset{k_2}{\underset{k_{-2}}{\rightleftharpoons}} \underset{6}{(H_2O)_4M\langle^{L}_{L}\rangle_{L}} + H_2O \quad (8)$$

$$\underset{6}{} \overset{k_3}{\underset{k_{-3}}{\rightleftharpoons}} \underset{MD}{(H_2O)_3M\langle^{L}_{L}\rangle_{L}} + H_2O \quad (9)$$

$$k_{ss} = \frac{K_0k_1k_2k_3}{k_{-1}k_{-2} + k_{-1}k_3 + k_2k_3} \quad (10)$$

The intermediate X (eq 1) that accumulates in our systems is most probably the bidentate intermediate **6**. If k_{-a} for **2** had a value as large as 0.1 s^{-1}, it would have been detected as a measurable intercept in the plots shown in Figure 3. If we use this value as an upper limit and the value of k_a at pH 8.3 (Table II) for completely ionized **2**, a lower limit of 10^4 is estimated for the formation constant of X from **2**. This lower limit is large for a unidentate complex but is comparable to the value for bidentate complexes of nickel with ligands such as malonic acid (log K_1 = 4.10)[13] and 3-aminobutanoic acid (log K_1 = 4.60).[14] If we assume a comparable upper limit for k_{-a} for **1**, an even larger lower limit on the formation constant of X from **1** is computed. If X is identified with **6**, the steady-state approximation can be applied to **5** if we make the further (justifiable) assumption that k_{-2} is negligibly small. The following identities are obtained:

$$k_{-a} = k_{-2} \qquad k_b = k_3 \quad (11)$$

$$k_a = K_0k_1\left(\frac{k_2}{k_{-1} + k_2}\right) \quad (12)$$

In eq 12, the factor in parentheses gives the fraction of **5** that is partitioned in the forward direction. The assumption that k_{-2} is negligible is justified by the facts that k_{-a} is negligible and that $k_{ss} = k_a$. The second fact requires that the $k_{-1}k_{-2}$ term in the denominator of eq 10 be negligible compared to the other two terms, so that eq 10 reduces to eq 12.

It is instructive now to compare the specific rate constants for particular dye species (Table III) with the estimated maximum values expected if the formation of the unidentate intermediate **5** were completely rate limiting. In this case k_a or k_{ss} would be equal to K_0k_1. We assign a value of 0.1 to K_0 for an uncharged ligand[15] and a value of 1–2 for a monoanion.[15,16] Assuming the I_d mechanism and equating k_1 to the water-exchange rate in Ni^{2+} (3×10^4 s^{-1}),[17] we obtained estimates of 3×10^3 and (3–6) $\times$ 10^4 M^{-1} s^{-1} for K_0k_1 for the neutral dye species and the monoanions, respectively. Comparison of these estimates with the experimental values shows that the monoanions of **1** and **2** react more slowly by factors of 50–100 and 25–50, respectively. The estimated upper limit for the rate constant for the neutral species of **1** is smaller than K_0k_1 by a factor of more than 200, and the experimental constant for the neutral species of **2** is smaller by a factor of more than 10^3. Space-filling models show no serious steric impediments to the initial bond formation with either dye, so we attribute the slow formation of the bidentate intermediate **6** to an unfavorable partitioning of the unidentate intermediate **5** in the direction of ring closure ($k_{-1} >> k_2$).

Table III also contains specific rate constants for the α-PAN dye **7** from an earlier study.[2] There is wide variation in reactivity

(11) Funahashi, S.; Tanaka, M. *Inorg. Chem.* **1969**, *8*, 2159.
(12) Cassatt, J. C.; Wilkins, R. G. *J. Am. Chem. Soc.* **1968**, *90*, 6045.
(13) Nair, V. S. K.; Nancollas, G. H. *J. Chem. Soc.* **1961**, 4367.
(14) Sharma, V. S.; Mathur, H. B.; Kulkarni, P. S. *Indian J. Chem.* **1965**, *3*, 475.
(15) Margerum, D. W.; Cayley, G. R.; Weatherburn, D. C.; Pagenkopf, G. K. In "Coordination Chemistry", Vol. 2; Martell, A. E., Ed.; American Chemical Society: Washington, DC, 1978; ACS Monogr. 174, p 13.
(16) Lin, C.-T.; Bear, J. L. *J. Phys. Chem.* **1971**, *75*, 3705.
(17) Connick, R. E.; Fiat, D. *J. Chem. Phys.* **1966**, *44*, 4103.

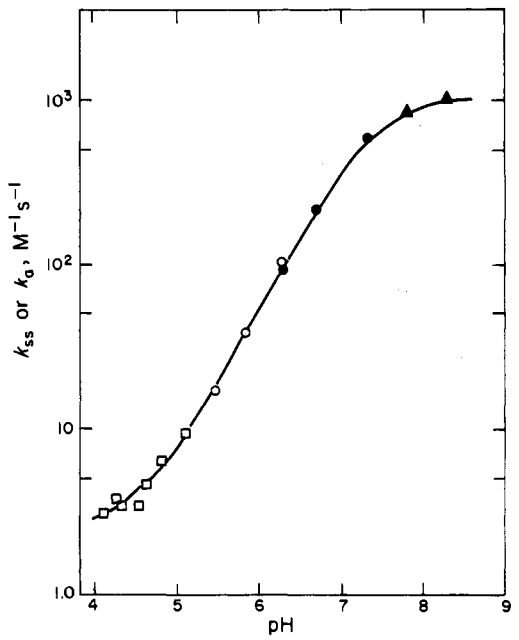

Figure 7. Semilog plot of k_{ss} (open points) or k_a (solid points) for dye **2** as a function of pH: □, acetate buffers; ○, MES buffers; ▲, HEPPS buffers. T = 25 °C; $[B^-]$ = 0.01 M; I = 0.1 M. The continuous line was calculated with eq 5 and the rate constants from Table III.

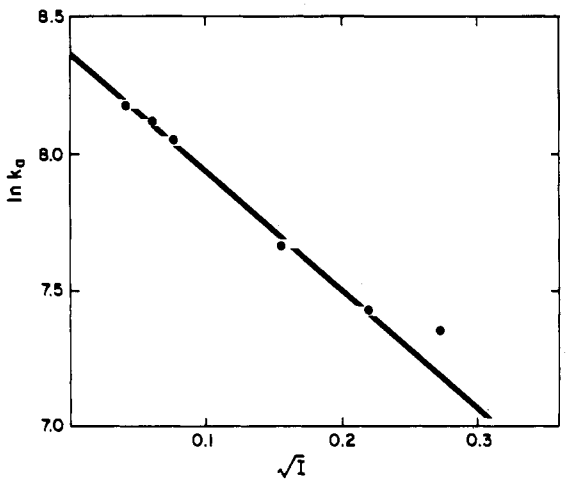

Figure 8. Plot of ln k_a for dye **2** as a function of $I^{1/2}$ in a pH 8.6 HEPPS buffer.

among the dyes when the same species are compared. The rate constants for both species of **7** are close to the maximum values estimated for K_0k_1, so there appears to be rapid ring closure of **5** and **6** for this dye. Hubbard and Pacheco pointed out this large difference in rates among dye ligands[18] and ascribed the slow rate of chelation of β-PAN (**8**) to the slow ring closure of **6**. They suggested that the slow rate resulted from the existence of a hydrogen-bonded tautomer that locked the dye into a conformation that was unfavorable for the final ring closure.

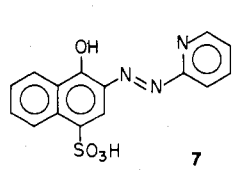

7

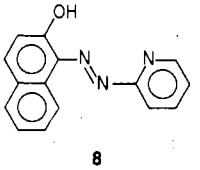

8

Our results suggest that at least two factors contribute to slow ring closure. The possibility of tautomerism is removed in the monoanions, and the rate retardations (Table III) must have a steric origin. Space-filling models show that the ligand groups in **1** and **2** are crowded in conformations required for chelate formation. Bond angles and distances appear to be distorted in the possible bidentate intermediates and the tridentate products. This is reflected in smaller stability constants for the 1:1 and 1:2 Ni:dye complexes of **1**[4] compared to those of other unhindered tridentate azo dyes such as **8**.[19] The ^1H NMR data show that at least some of the possible conformations do not interconvert rapidly on the NMR time scale at room temperature. In addition, **1** and **2** can form either of two 6–5 chelates, and we do not know which is the more stable. Models show that formation of either requires that the dye assume a hindered or strained conformation in order to close the second ring. We attribute the slow rate to a very low equilibrium population of the necesary conformation. In addition, it is possible that the bidentate intermediate that forms fastest could lead to the most strained product if ring closure continued. In this event, formation of the final product might require the rearrangement of the bidentate intermediate,[20] which would probably be slow because it requires the opening of a bidentate chelate ring. These problems do not arise with **7** because there can be only one 5–5 chelate, and steric constraints appear to be absent in the conformations required to form intermediates and products.

Table III shows that the differences between experimental rate constants and the appropriate estimates of K_0k_1 are greater for the undissociated dyes than for their monoanions. If we assume that the steric constraints are about the same in both forms, an additional contribution to slow ring closure is needed that is characteristic of the undissociated dyes alone. We suggest that this added factor is the existence of tautomeric forms. The spectral results show that the hydrazone tautomer (**A**, Scheme I) is the predominant form of the undissociated dyes. As a hypothesis we assume that both hydrazone and azo enol (**B**) forms undergo initial ligation but the **B** tautomer undergoes more rapid ring closure. An extreme case is shown as follows, where the hydrazone tautomer does not react beyond the initial ligation and chelation occurs only via the **B** tautomer in equilibrium with **A**:

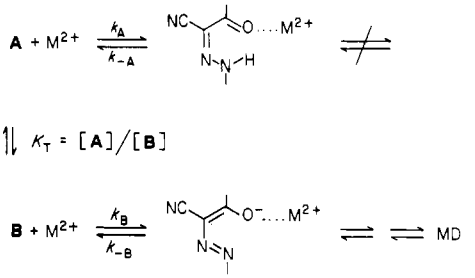

If the tautomeric equilibrium is established rapidly, the steady-state approximation to all intermediates gives

$$k_{Ni^{2+},DH} = \frac{K_0k_1k_2k_3}{K_T(k_{-1}k_{-2} + k_{-1}k_3 + k_2k_3)} \qquad (13)$$

More complex rate expressions are obtained by assuming that the hydrazone reacts but at a slower rate than the azo enol tautomer; however, eq 13 is sufficient to show that with the stated hypothesis a large value of K_T gives a small experimental rate constant, other things being equal.

There are two possible reasons that the hydrazone form might undergo slower ring closure. The first involves hydrogen bonding in the hydrazone tautomer that constrains the dye into an unfavorable conformation, as suggested by Hubbard and Pacheco.[18] This factor could contribute regardless of which of the two possible nitrogens in the azo bridge is ultimately involved in the final stable chelate. A second possibility is that the mere presence of the hydrogen on a nitrogen atom that is required in the chelate formation could inhibit bond formation to that nitrogen. In this case, not all hydrazones would show retardation.

(18) Hubbard, C. D.; Pacheco, D. *J. Inorg. Nucl. Chem.* **1977**, *39*, 1373.

(19) Corsini, A.; Yih, I. M.-L.; Fernando, Q.; Freiser, H. *Anal. Chem.* **1962**, *34*, 1090.

(20) We are indebted to Professor D. W. Margerum for this suggestion.

The undissociated form of dye **7** exists largely as the quinone hydrazone, and consideration of its geometries is instructive in view of its high reactivity. The nitrogen adjacent to the naphthalene ring becomes bonded to the metal ion in the 5-5 chelate, and conformation **G** is required ultimately for chelate formation.

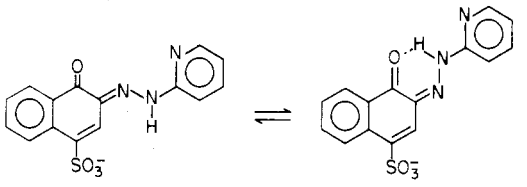

G **H**

The nitrogen with the attached proton is not involved. On the other hand, conformation **H** results if the hydrazone is hydrogen bonded, and conversion to **G** requires the breaking of the bond coupled with isomerization. The high reactivity of the undissociated form of **7** suggests that the hydrogen-bonding possibility is not important with this dye.

The possibility of forming two 6-5 chelates may account for the slow equilibration in **1** after the initial chelation. If the less stable chelate forms more rapidly, the reequilibration to the more stable chelate would be slow because of the need to open and rearrange a tridentate chelate.

Acknowledgment. We are indebted to Professors D. W. Margerum and W. P. Jencks for helpful discussions of this work and to our Kodak colleagues for the dyes.

Registry No. **1**, 94499-10-2; **2**, 94499-11-3; Ni, 7440-02-0.

Contribution from the Research Laboratories and Kodak Park Division, Eastman Kodak Company, Rochester, New York 14650

Application of Factor Analysis to the Spectrophotometric Determination of Formation Constants of Complexes of Nickel(II) with Tridentate Dyes

RICHARD L. REEVES,* MARY S. MAGGIO, SHELLEY A. HARKAWAY, and GREGG A. MEYERS

Received April 18, 1984

Absorption curves of solutions containing a dye ligand and its 1:1 and 1:2 nickel(II) complexes have been analyzed by factor analysis to extract the (often) inaccessible absorption curve of the 1:2 complex and its formation constant, K_2. The method was applied to an *o,o'*-dihydroxy phenylazo dye, Solochrome Violet (SV), and to two α-[(2-hydroxyphenyl)azo]-α-acetoacetonitrile dyes. Required inputs are a family of absorption curves containing various proportions of the dye and two complexes, reference curves for the dye and the 1:1 complex, the pK_a's of the ligand groups, and an independently determined value of the formation constant of the 1:1 complex, K_1. The derived value of K_2 for SV agreed with the value determined earlier by potentiometric titration. The method was successful in cases where the absorption curves of the two complexes showed small differences in shape and/or λ_{max} but failed where the two curves differed only in amplitude. The values of K_1 and K_2 for the acetoacetonitrile dyes are smaller by several orders of magnitude than those of related dyes; the spectra and molecular models suggest that bond angles and lengths are distorted in the chelates. The advantages and disadvantages of the approach are discussed.

This paper describes a useful method for estimating formation constants of 1:2 complexes of metal ions and tridentate dye ligands from the spectra of three-component mixtures and its application to some dyes of interest in mechanistic studies.[1] Few constants for 1:2 complexes of such dyes have been reported. In appropriate applications the method has some advantages over other methods. The disadvantage of the potentiometric method in water is that the dyes are usually aggregated at concentrations where useful titrations can be made.[2,3] The effort required to correct for the aggregation can be greater than that involved in measuring the stability constants.[4] Spectrophotometric methods allow measurements at dye concentrations where aggregation is not a problem. The spectral methods have increased in sophistication from those that utilize absorbance changes at a single wavelength to computer-assisted regression and matrix methods that treat data at multiple wavelengths.[5-10] The latter approach is highly desirable in the present application because the absorption curves of the 1:1 and 1:2 metal:dye complexes can be quite similar, and an equilibrium model that fits data at a single wavelength may fail when constrained to describe data at a number of wavelengths. Thus, the complexation of copper(II) with a bidentate azo dye is reported to give only two absorbing species[11] by application of the molar ratio,[12] Job's,[13] straight line,[14] and slope ratio[15] methods to data at a given wavelength, whereas inspection of the complete absorption curves suggests that additional species are probably present.

The application of factor analysis[16-18] to a family of absorption curves made up of various contributions of components in equilibrium utilizes all the information in the absorption curves and can, in principle, yield simultaneous estimates of an equilibrium constant and an unknown or inaccessible absorption curve. The successful application of the method of analysis to a study of the aggregation of azo dyes in water,[3] where differences in the absorption curves of monomers, dimers, and *n*-mers are small, led us to try it with metal–dye complexation equilibria. In this paper we describe a study of the formation constants for the 1:1 (K_1)

* To whom correspondence should be addressed at the Research Laboratories.

(1) Meyers, G. A.; Michaels, F. M.; Reeves, R. L.; Trotter, P. J. *Inorg. Chem.*, preceding paper in this issue.
(2) Coates, E.; Rigg, B. *Trans. Faraday Soc.* **1961**, *57*, 1637.
(3) Reeves, R. L.; Maggio, M. S.; Harkaway, S. A. *J. Phys. Chem.* **1979**, *83*, 2359.
(4) Coates, E.; Rigg, B. *Trans. Faraday Soc.* **1962**, *58*, 2058.
(5) Coleman, J. S.; Varga, L. P.; Mastin, S. H. *Inorg. Chem.* **1970**, *9*, 1015.
(6) Grabaric, B.; Piljac, I.; Filipovic, I. *Anal. Chem.* **1973**, *45*, 1932.
(7) Sommer, L.; Havel, J. *Collect. Czech. Chem. Commun.* **1977**, *42*, 2134.
(8) Voznica, P.; Havel, J.; Sommer, L. *Collect. Czech. Chem. Commun.* **1980**, *45*, 54.
(9) Suchanek, M.; Sucha, L. *Collect. Czech. Chem. Commun.* **1978**, *43*, 1393.
(10) Meloun, M.; Chylkova, J.; Panel, J. *Collect. Czech. Chem. Commun.* **1978**, *43*, 1097.
(11) Khalifa, H.; Barsoum, B. N.; El-Gazzar, E. A. *Microchem. J.* **1980**, *25*, 429.
(12) Yoe, J. H.; Jones, A. L. *Ind. Eng. Chem., Anal. Ed.* **1944**, 111.
(13) Vosburgh, W. C.; Cooper, G. R. *J. Am. Chem. Soc.* **1941**, *63*, 437.
(14) Asmus, E. I. *Z. Anal. Chem.* **1960**, *178*, 104.
(15) Harvey, A. E., Jr.; Manning, D. L. *J. Am. Chem. Soc.* **1950**, *72*, 4488.
(16) Kowalski, B. R., Ed. "Chemometrics. Theory and Practice"; American Chemical Society: Washington, DC, 1977; ACS Symp. Ser. No. 52.
(17) Rummel, R. J. "Applied Factor Analysis"; Northwestern University Press: Evanston, IL, 1970.
(18) Weiner, P. H. *CHEMTECH* **1977**, *7*, 321.

0020-1669/85/1324-0738$01.50/0